GEOPHYSICAL RESEARCH LETTERS, VOL. 37, L04105, doi:10.1029/2009GL041541, 2010

An investigation of the association between steady magnetospheric convection and CIR stream interfaces

J. Kissinger,[1] R. L. McPherron,[2] V. Angelopoulos,[2] T.-S. Hsu,[2] and J. P. McFadden[3]

Received 16 November 2009; revised 13 January 2010; accepted 22 January 2010; published 27 February 2010.

[1] It has been postulated that steady magnetospheric convection (SMC), a mode of response of the Earth's magnetosphere to solar wind driving, is caused by balanced day and night side reconnection. We investigate this possibility with a statistical study of return flows in the magnetotail during SMC using the THEMIS mission. Between December 2007 to April 2009, 153 events were identified. We find flows greater than 100 km/s throughout the magnetotail but no distinct pattern of flow channels. SMC occurrence is compared with that of stream interfaces (SI) at the center of corotating interaction regions. "Frequent" SMCs are observed ±1 day around the SI, and "infrequent" 3 to 1.5 days before the SI. The typical solar wind parameters in the frequent interval are higher than expected from previous studies. We found that rectified solar wind electric field steadiness predicts that SMC will occur when this is smaller than average. **Citation:** Kissinger, J., R. L. McPherron, V. Angelopoulos, T.-S. Hsu, and J. P. McFadden (2010), An investigation of the association between steady magnetospheric convection and CIR stream interfaces, *Geophys. Res. Lett.*, *37*, L04105, doi:10.1029/2009GL041541.

1. Introduction

[2] During moderate steady driving of the Earth's magnetosphere by the solar wind, a mode of response called steady magnetospheric convection (SMC) or convection bays can occur [*Pytte et al.*, 1978]. This response is characterized by enhanced convection in the magnetosphere and ionosphere without any substorm expansions [*Sergeev et al.*, 1996]. *Dungey* [1961] first described a system in which southward interplanetary magnetic field (IMF) causes magnetic reconnection with the Earth's magnetic field at the dayside subsolar region of the magnetopause. This creates open field lines, allowing solar wind energy into the magnetosphere. The solar wind forces these lines up and over the polar caps into the tail, stretching out the field lines. Flux and magnetic pressure build up, thinning the plasma sheet, until a second near-Earth x-line at 15–25 R_E is formed, closer than the distant x-line at ~100 R_E. A plasmoid moves down the tail, and energy and magnetic flux flows Earthward and returns to the dayside, crossing both dawn and dusk terminators. Pileup exerts pressure on the near-Earth x-line, causing it to move down the tail. This is a classic substorm [*Baker et al.*, 1996]. SMC events typically begin with a substorm, but instead of the x-line retreating to 100 R_E, it moves to an intermediate distance and stays there. It has been proposed that during SMC, opening flux by dayside reconnection and closing flux with nightside reconnection are relatively balanced [*Pytte et al.,* 1978; *DeJong and Clauer,* 2005; *DeJong et al.*, 2007; *McWilliams et al.*, 2008].

[3] If it is indeed the case that flux is returning to the dayside fast enough to balance the erosion there, we expect to see fast filamented convection flows in the tail, as observed and depicted by *Sergeev et al.* [1990, 1996, Figure 17]. With this motivation, we searched for SMC events while the THEMIS spacecraft were in the magnetotail, and then investigated whether high-speed flows were seen by the spacecraft.

[4] SMCs are just one way the magnetosphere can respond to solar wind driving; substorms and sawtooth events are also modes of response. Why does the magnetosphere enter into one mode instead of another? The average solar wind conditions favorable to SMC are known: slow solar wind speed (350 km/s) and moderate, stable IMF B_z (−3 nT) [*McPherron et al.*, 2005]. However, *O'Brien et al.* [2002] showed that similar solar wind conditions can produce either a substorm or an SMC. To better understand how solar wind changes can result in SMC, we compared our list of SMC events with a list of stream interfaces within corotating interaction regions to determine if there is any correlation.

2. Selection of SMCs

[5] Our event selection primarily used the procedure described by *O'Brien et al.* [2002], who identified events from auroral indices. SMC events were chosen by visual inspection of the AE (auroral electrojet) index, made up of AL and AU indices. We required 1) AU > 50 nT and AL < −75 nT; 2) the change in the AL index dAL/dt (a 15 minute sliding derivative operator) be within 10 nT/min > dAL/dt > −7.4 nT/min; 3) the event last longer than 90 minutes; and 4) at least 90% of points in a given interval satisfy all the above criteria. The limits were selected to be larger than the magnitude of a quiet day (±50 nT), but low enough so small SMCs would be selected. One hundred and fifty-three intervals satisfying these criteria were identified between December 2007 to July 2008, and from November 2008 to April 2009.

[6] An example of an SMC interval is shown in Figure 1. The event occurred on 24 January 2008. The first panel shows the AU and AL indices. AU is a measure of the eastward electrojet strength, and AL is a measure of the westward electrojet strength. The event is preceded by a substorm, after which enhanced, steady AL continues for about four hours.

[1]Department of Earth and Space Sciences, University of California, Los Angeles, California, USA.
[2]Institute of Geophysics and Planetary Physics, University of California, Los Angeles, California, USA.
[3]Space Sciences Laboratory, University of California, Berkeley, California, USA.

0094-8276/10/2009GL041541$05.00

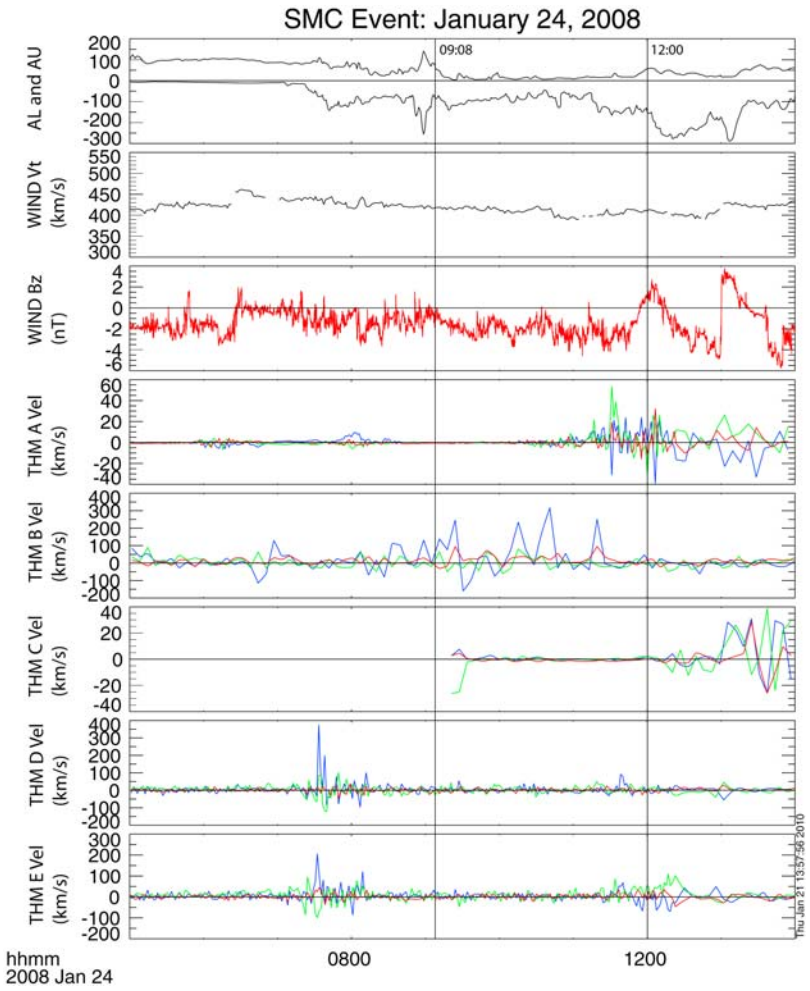

Figure 1. A typical SMC event on 1/24/2008. Plotted are Kyoto AU and AL indices, WIND solar wind total velocity (V_t) and WIND magnetic field (B_z) in GSE coordinates. The remaining panels are the three velocity components of all five THEMIS spacecraft (x, y, and z are blue, green, and red respectively). Flows are seen at SMC start at THEMIS D and E, and continuously throughout the SMC at THEMIS B.

Solar wind speed (panel 2) remains steady at around 425 km/s, slowly decreasing over the interval. IMF B_z (panel 3) goes negative before the interval, and stays mostly negative throughout the SMC (−2 nT). The northward turning just before 12:00 UT causes the SMC to terminate in another substorm. The remaining panels show THEMIS ESA velocity data [*McFadden et al.*, 2008] from five spacecraft within the magnetotail; at THEMIS B (x = −20 R_E), strong Earthward flows are seen throughout the interval, while THEMIS D and E (x = −10 R_E, toward dawn) only see flows during the substorm before the SMC.

3. Return Flows in the Magnetotail during SMC

[7] We looked for high speed flow bursts in THEMIS ESA (Electrostatic analyzer) data during SMC intervals. A burst was 'fast' if $V_{x,GSM}$ was greater than 100 km/s. All five THEMIS spacecraft were included in the survey, but only when in the magnetotail. Figure 2 depicts all flow bursts in the x-y GSM (Geocentric Solar Magnetospheric) coordinate plane. If there were several flow bursts at a spacecraft during an SMC interval, the average of those bursts is plotted. Blue arrows show earthward flows, and

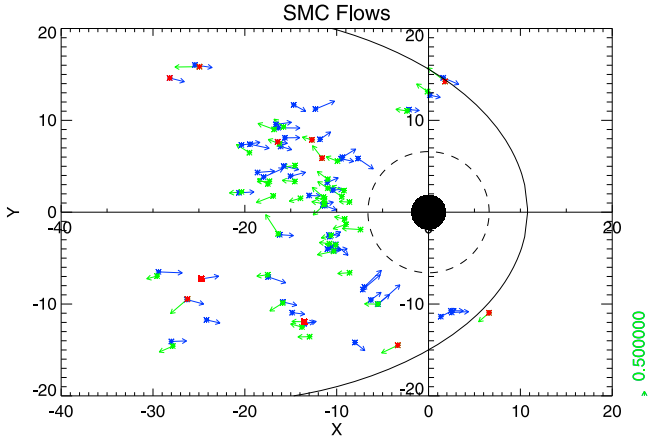

Figure 2. Fast flows in the Earth's magnetotail during SMC intervals as seen by THEMIS. Blue arrows are earthward flows, green are tailward. Multiple flows were averaged together. A red dot at the base indicates that B_z is negative. The dotted circle is geosynchronous orbit, and the black curve is the magnetopause.

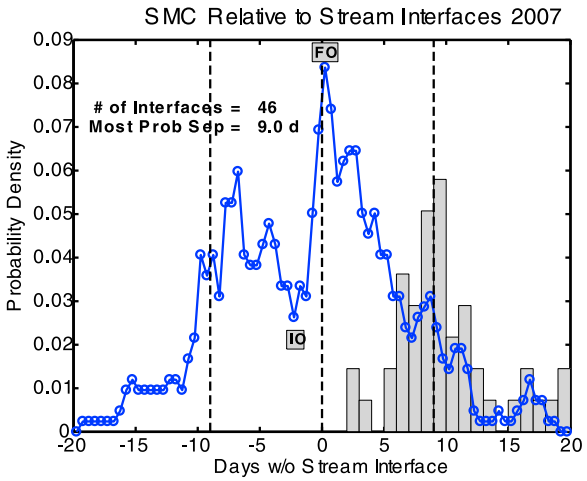

Figure 3. SMC intervals were compared with stream interfaces (SI). An SI is marked as t = 0 days (middle dashed black line), and occurrence of SMCs in the days before and after is plotted in half-day intervals as probability density (blue line with circles). A bar graph centered at 9.0 days is a histogram of separation between successive SI. Vertical dashed lines to the left and right represent the average time between adjacent SI. FO shows frequent SMC occurrence, and IO infrequent.

green arrows show tailward flows. A red dot at the base of a flow indicates that the average magnetotail B_z during the flow was negative, and thus the spacecraft is tailward of the x-line. The dashed black circle is geosynchronous orbit (6.6 R_E), and the black curve corresponds to a typical magnetopause.

[8] Both tailward and earthward flows appear throughout the tail at almost the same frequency. No obvious flow channels are seen. Very few cases of southward magnetotail B_z (red dot) are seen with the tail flows. In fact there is little evidence of flows approaching the terminators. It may be that the tail flux moves quickly in the more distant tail, piles up in a region at around 7–8 R_E, and continues around the Earth at a slower pace to finally reach the dayside reconnection region. *Lopez et al.* [2008] have used LFM simulations of steady storms and found that fast, prolonged sunward flows may move just inside the magnetosphere in the low latitude boundary layer (LLBL). Expansion of our study to times when THEMIS spacecraft were along the terminators could help determine if this is the case.

4. Correlation Between SMCs and CIRs

[9] A stream interface (SI) is a region of interaction between slow and fast speed streams, emanating from the Sun. These regions are also known as "corotating interaction regions" (CIRs) as they corotate with the Sun, and the SI within is characterized by a sharp decrease in density and increase in velocity. Prior to the SI, typical solar wind conditions include high density, slow and steady velocity, and steady IMF. After the SI, the solar wind is fast and tenuous, and fluctuations in velocity and field increase [*Gosling et al.*, 1978]. CIRs are highly structured, systematic sequences that organize activity in the magnetosphere, such as relativistic electron growth. The possibility that they organize other activity motivated us to investigate the relationship of SMC events to SI.

[10] We compared our SMC event list to a list of SIs identified during the THEMIS mission. For each SI we selected only those SMC that occurred after the preceding SI and before the following one. We calculated the delay of SMC onset relative to the time of the current SI. The delays were accumulated and a histogram was constructed with 12-hour bins for 20 days before and after the time of SI. Note that a positive delay for one interface will become a negative delay for the next interface, effectively doubling the number of events. If all SIs were separated by exactly the same amount of time (i.e. 7 days) no SMC would occur before the preceding interface (−7 days) or after the following interface (+7 days). In our case the average time between SIs was nine days, but the typical variation in this number was about two days. This contributes some counts before and after the average SI time separation. Nine days after the largest peak, we see a small second peak in SMC occurrence, a half day before the average time of the "next SI". We do not expect an exact repetition of the central peak because of the variability of the time between interfaces.

[11] Figure 3 summarizes the correlation between SMC occurrence and SIs. The abscissa shows the number of days before and after a SI. The solid blue line with circles shows the probability density of SMC seen in half-day intervals (0 to 0.5 days, 0.5 to 1 days, etc) relative to the SI. The middle vertical dashed line (t = 0) is the time of the SI used in calculating time delays. Vertical dashed lines to the left and right represent the average time between adjacent interfaces. A bar graph centered at +9.3 days is a histogram of the time delays to the next SI, and the annotation on the graph lists properties of this histogram.

[12] It is evident that more SMC occur during the CIR than just before it arrives. The highest probability of observing an SMC is 12 hours immediately after the SI. A minimum in SMC occurs 24–36 hours before the SI. These results were also verified using superposed epoch analysis. We have used this higher resolution analysis to define two intervals of SMC occurrence relative to the SI. The infrequent (IO) interval is −2.8431 to −1.4465 days and the frequent (FO) interval is −0.7847 to 1.2840 days. These intervals are used in our subsequent analysis.

[13] Solar wind data were separated into infrequent and frequent intervals. Each interval was then further split into data when SMCs actually occurred, and 'everything else' when SMCs did not occur. This resulted in four classes: (1) frequent SMC occurrence, with SMC (F-Occ); (2) frequent SMC occurrence, no SMC (F-Non); (3) infrequent SMC occurrence, with SMC (I-Occ); and (4) infrequent SMC occurrence, no SMC (I-Non).

[14] Cumulative probability distributions were calculated for various solar wind parameters and their fluctuations. Figure 4 displays V_t, IMF B_z, electric field (E_s; rectified E_y), and normalized E_s fluctuations, or steadiness. Steadiness (coefficient of variance) is found by dividing a running hourly standard deviation of E_s by a running hourly mean of E_s [*DeJong et al.*, 2009]. Solid red lines correspond to F-Occ, solid blue to I-Occ, magenta lines with diamonds correspond to F-Non, and cyan with squares to I-Non. Black dotted lines denote the value at which the two solid curves (F-Occ and I-Occ) have maximum separation; the plot annotations show this value (V_{mx}) and the

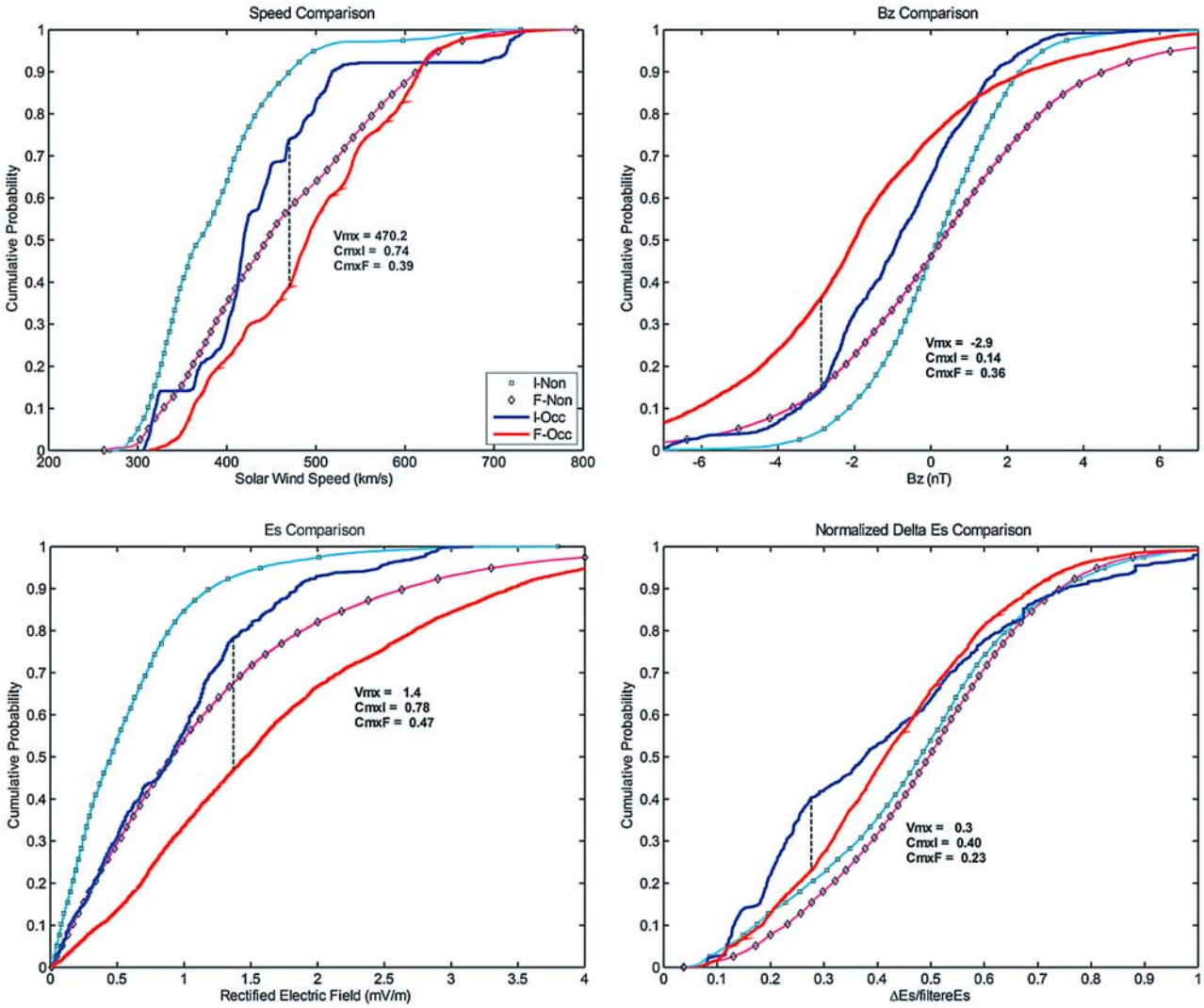

Figure 4. Probability distribution functions of solar wind (top left) V_t, (top right) B_z, (bottom left) electric field E_s, and (bottom right) E_s steadiness. F-Occ are solid red lines; I-Occ are solid blue; F-Non are magenta with diamonds; and I-Non is cyan with squares.

corresponding probabilities (C_{mxI} for infrequent/blue, C_{mxF} for frequent/red). Density and density steadiness is the same regardless of whether SMC are occurring or not, and are not shown.

[15] V_t is higher during the frequent interval than infrequent. For both intervals, V_t is higher during times when SMCs are occurring than when SMCs do not occur. Average V_t during SMCs is 500 km/s (frequent). However, *O'Brien et al.* [2002] found that V_t during SMCs is less than 450 km/s. Furthermore, *DeJong et al.* [2009] show that V_t is smaller during SMCs compared to the background, and that less than 1% of all SMCs occur for $V_t > 500$ km/s. The cdf of V_t during all SMCs (not shown) follows the same trend as F-Occ, where nearly half of SMC times correspond to $V_t > 500$ km/s. Thus the SMC events that occur near a SI correspond to much higher V_t than expected. V_t steadiness does not differ between SMC and non-SMC times.

[16] B_t (not shown) is stronger for frequent than the infrequent interval. Similarly the frequent interval has stronger B_z. When SMC are occurring, solar wind B_z is more negative. The steadiness of B_z is identical during SMC and non-SMC occurrence; thus SMC occurrence does not depend on fluctuations in B_z. Results from *DeJong et al.* [2009] indicate that B_z should be more steady during SMC. In our case, the hourly averaged standard deviation of B_z is actually normalized by hourly averaged B_t, and thus the difference could be explained by a B_y effect. We also used a 1-hour interval instead of the 30 minute period used by DeJong *et al.*, which may average out fluctuations.

[17] Most of our SMCs occur during relatively weak electric field. The frequent interval dominates, biased in the direction expected for its position in the CIR. For both intervals, E_s is larger when SMC are observed. The fluctuations in E_s (not shown) are much larger during the CIR than before it arrives, and in both intervals fluctuations are larger when SMC are occurring. However, E_s steadiness shows that in both intervals, when SMC are occurring E_s is steadier. SMC occur in steadier electric field. This matches

previous studies which showed that SMC events occur when the solar wind is more stable [*McPherron et al.*, 2005; *DeJong et al.,* 2009].

5. Conclusions

[18] We searched for evidence of fast flows in the magnetotail during SMC events. We found 54 fast earthward flows and 47 tailward flows. The existence of flow channels back to the dayside was inconclusive. The average speed of earthward flows (166 km/s) is slightly faster than the average tailward flows (151 km/s). In about 40% of the cases, a spacecraft saw both high velocity earthward and tailward flows during one event, but there was no order to the association (i.e., neither earthward-then-tailward or tailward-then-earthward dominated). It may be that the plasma is moving along just inside the magnetosphere in the LLBL. In a further study we will include THEMIS passes through the dawn and dusk flanks, to search for flows in the LLBL.

[19] The correlation between CIRs and the magnetosphere entering SMC was not previously known. We searched for possible control by the Russell-McPherron effect [*Russell and McPherron*, 1973] by classifying the IMF spiral angle during all SMC events according to the "Spring To, Fall Away" rule, but found no significant role. For the high occurrence of SMCs at the SI, the only causative factor we found is steady E_s. There is an equal probability of steadier E_s in both the infrequent and frequent interval, but solar wind driving is not strong enough to generate magnetospheric activity during the infrequent interval. Driving increases with the arrival of the SI, and generates more measurable activity.

[20] SMC intervals that occur near CIRs differ from what is expected from previous studies: V_t is higher, and B_z steadiness shows no difference from background levels. A possible difference between our results and others could be due to the solar cycle. While our events were in the descending and minimum (DN) phase (2007–2009), *DeJong et al.* [2009] had events from 1997–2002, the ascending and maximum (AX) phase of the solar cycle. During DN phases, high speed streams are more commonly observed [*Gosling et al.,* 1971; *Leinert and Jackson,* 1998]. These higher solar wind parameters could result in a subset of SMCs within solar minimum of pre- and post-SI conditions where solar wind parameters are higher than usual, but not strong enough to result in a substorm. Although *McPherron et al.* [2005] examined SMCs over an entire solar cycle, they did not examine the properties of SMCs in different parts of the solar cycle; this subset of solar minimum SMCs may have been averaged out in their results. Future work should examine the differences in SMC events by solar cycle phase.

[21] **Acknowledgments.** We thank the World Data Center for Geomagnetism, Kyoto for the use of provisional AL and AU data. This paper is based upon work supported by the National Science Foundation under Agreement Number ATM-0720422 and by NASA NNX07AG16G. We acknowledge the THEMIS program, supported by NASA contract NAS5-02099, and C. W. Carlson and J. P. McFadden for use of ESA data.

References

Baker, D. N., T. I. Pulkkinen, V. Angelopoulos, W. Baumjohann, and R. L. McPherron (1996), Neutral line model of substorms: Past results and present view, *J. Geophys. Res.*, *101*, 12,975–13,010.

DeJong, A. D., and C. R. Clauer (2005), Polar UVI images to study steady magnetospheric convection events: Initial results, *Geophys. Res. Lett.*, *32*, L24101, doi:10.1029/2005GL024498.

DeJong, A. D., X. Cai, R. C. Clauer, and J. F. Spann (2007), Aurora and open magnetic flux during isolated substorms, sawteeth, and SMC events, *Ann. Geophys.*, *25*, 1865–1876.

DeJong, A. D., A. J. Ridley, X. Cai, and C. R. Clauer (2009), A statistical study of BRIs (SMCs), isolated substorms, and individual sawtooth injections, *J. Geophys. Res.*, *114*, A08215, doi:10.1029/2008JA013870.

Dungey, J. W. (1961), Interplanetary magnetic field and the auroral zones, *Phys. Rev. Lett.*, *6*(2), 47–48, doi:10.1103/PhysRevLett.6.47.

Gosling, J. T., R. T. Hansen, and S. J. Bame (1971), Solar wind speed distributions: 1962–1970, *J. Geophys. Res.*, *76*, 1811–1815, doi:10.1029/JA076i007p01811.

Gosling, J. T., J. R. Asbridge, S. J. Barne, and W. C. Feldman (1978), Solar wind stream interfaces, *J. Geophys. Res.*, *83*, 1401–1412, doi:10.1029/JA083iA04p01401.

Leinert, C., and B. V. Jackson (1998), Global solar wind changes over solar cycle 21: A combination of Helios photometer, in situ, and interplanetary scintillation data, *Astrophys. J.*, *505*, 984–992, doi:10.1086/306180.

Lopez, R. E. (2008), THEMIS observations of boundary layer flows during a storm: Evidence for the quasi- stable storm reconnection region, *Eos Trans. AGU*, *89*(23), West. Pac. Geophys. Meet. Suppl., Abstract SP23A-04.

McFadden, J. P., C. W. Carlson, D. Larson, M. Ludlam, R. Abiad, B. Elliott, P. Turin, M. Marckwordt, and V. Angelopoulos (2008), The THEMIS ESA plasma instrument and in-flight calibration, *Space Sci. Rev.*, *141*, 277–302, doi:10.1007/s11214-008-9440-2.

McPherron, R. L., T. P. O'Brien, and S. M. Thompson (2005), Solar wind drivers for steady magnetospheric convection, in *Multiscale Coupling of the Sun-Earth Processes*, edited by A. T. Y. Liu, Y. Kamide, and G. Consolini, pp. 113–124, Elsevier, Amsterdam.

McWilliams, K. A., J. B. Pfeifer, and R. L. McPherron (2008), Steady magnetospheric convection selection criteria: Implications of global SuperDARN convection measurements, *Geophys. Res. Lett.*, *35*, L09102, doi:10.1029/2008GL033671.

O'Brien, T. P., S. M. Thompson, and R. L. McPherron (2002), Steady magnetospheric convection: statistical signatures in the solar wind and AE, *Geophys. Res. Lett.*, *29*(7), 1130, doi:10.1029/2001GL014641.

Pytte, T., R. L. McPherron, E. W. Hones Jr., and H. I. West Jr. (1978), Multiple-satellite studies of magnetospheric substorms: Distinction between polar magnetic substorms and convection-driven negative bays, *J. Geophys. Res.*, *83*(A2), 663–679, doi:10.1029/JA083iA02p00663.

Russell, C. T., and R. L. McPherron (1973), Semiannual variation of geomagnetic activity, *J. Geophys. Res.*, *78*(1), 92–108, doi:10.1029/JA078i001p00092.

Sergeev, V. A., O. A. Aulamo, R. J. Pellinen, M. K. Vallinkoski, T. Bosinger, C. A. Cattell, R. C. Elphic, and D. J. Williams (1990), Non-substorm transient injection events in the ionosphere and magnetosphere, *Planet. Space Sci.*, *38*(2), 231–239, doi:10.1016/0032-0633(90)90087-7.

Sergeev, V. A., R. J. Pellinen, and T. I. Pulkkinen (1996), Steady magnetospheric convection: a review of recent results, *Space Sci. Rev.*, *75*, 551–604, doi:10.1007/BF00833344.

V. Angelopoulos, T.-S. Hsu, and R. L. McPherron, Institute of Geophysics and Planetary Physics, University of California, Los Angeles, CA 90095, USA.

J. Kissinger, Department of Earth and Space Sciences, University of California, Los Angeles, CA 90095, USA. (jkissinger@ucla.edu)

J. P. McFadden, Space Sciences Laboratory, University of California, Berkeley, CA 94720, USA.